World Journal of Advanced Engineering Technology and Sciences
eISSN: 2582-8266
Cross Ref DOI: 10.30574/wjaets
Journal homepage: https://wjaets.com/

(RESEARCH ARTICLE)

Check for updates

Enhancing power flow control in double circuit transmission line using GWO-optimized pi controller for five level UPFC

Jayachandra R * and Tulasi Ram Das G

Department of Electrical and Electronics Engineering, Jawaharlal Nehru Technological University Hyderabad, India.

World Journal of Advanced Engineering Technology and Sciences, 2025, 14(03), 001-024

Publication history: Received on 15 January 2025; revised on 26 February 2025; accepted on 01 March 2025

Article DOI: https://doi.org/10.30574/wjaets.2025.14.3.0095

Abstract

Power flow control in double circuit transmission lines is crucial for maintaining system stability and ensuring optimal utilization of resources. This paper proposes a novel approach using a Five Level Unified Power Flow Controller (UPFC) with a Grey Wolf Optimizer (GWO) tuned Proportional-Integral (PI) controller. The Five Level UPFC acts as a flexible and efficient solution, facilitating the concurrent regulation of both active and reactive power flow in transmission lines. By applying the GWO algorithm, the aim is to improve the performance of the UPFC control system through the optimization of the PI controller's parameters. By imitating the natural hunting behaviour of grey wolves, the GWO algorithm achieves exceptional convergence and solution accuracy. The suggested control scheme is implemented and tested on a double circuit transmission line system. The system's effectiveness is evaluated under various operating conditions and compared against alternative control approaches. The findings establish the efficacy of the Five Level UPFC with a GWO-optimized PI controller in effectively regulating power flow and enhancing overall system stability. Furthermore, the proposed approach exhibits excellent robustness against parameter variations, load fluctuations, and system disturbances. The GWO optimization technique ensures optimal tuning of the PI controller, this leads to decreased power losses, enhanced voltage profile, and improved system reliability. Overall, the application of the Five Level UPFC with GWO-tuned PI controller provides an efficient and reliable solution for power flow control in double circuit transmission lines. The suggested method can make a substantial contribution to enhancing the operational efficiency of power systems, this enables the seamless integration of renewable energy sources and the progression of smart grid infrastructures. The circuit is simulated using the MATLAB/SIMULINK software. And the following results from the simulation are presented below

Keywords: UPFC; GWO; SCCS; STATCOM; THD

1. Introduction

Lately, there has been a growing significance placed on the preservation of reliable electric power for both electric utility companies and customers. Disturbances occurring on the utility and customer-side can cause voltage fluctuations, transients, and waveform distortions at the terminal, such conditions can result in adverse effects on the electric grid, leading to concerns regarding power quality. Power quality (PQ) refers to the maintenance of voltage and current

waveforms at the desired frequency and magnitude, retaining their original sinusoidal form [1]. As power electronic devices are increasingly integrated into various equipment, power systems have become more susceptible to power quality issues. Consequently, ensuring power quality has emerged as a crucial consideration in contemporary times. Power quality is influenced significantly by non-linear loads, which encompass power electronic devices, variable speed drives, and electronic control gears. Inadequate power quality has the potential to undermine the secure, dependable, and efficient functioning of equipment. Voltage sags, voltage swells, voltage fluctuations, voltage imbalances, and harmonics are among the various factors that fall under power quality concerns [2].

* Corresponding author: R. Jayachandra.

Progresses in power electronic devices have brought about significant developments in the field, Specifically, power quality has gained significant importance in domains like FACTS and devices for customized power solutions., has led to significant advancements, have given rise to a new field of technology that offers the power system enhanced control capabilities, leading to enhancements in power quality. The present power system is deregulated, with separate generation, transmission, and distribution systems producing electricity to provide cheaper power [3]. As the demand for electric power continues to grow, ensuring system stability, it becomes imperative to optimize the utilization of current generating units and maximize the load on existing transmission lines within their thermal limits. Minimizing transmission line losses is another important phase of power system operation [4]. The utilization of FACTS devices is crucial for power control and optimizing the operational capacity of existing transmission lines.

The utilization of power electronic components in FACTS devices enhances control capabilities and augments the power transfer capacity. By integrating FACTS devices into the electric transmission system, it has the potential to revolutionize the future of the system, transforming it into a more intelligent and advanced infrastructure [5]. FACTS controllers such as STATCOM, TCSC, SSSC, and SVC enable rapid and efficient regulation of network conditions. This, in turn, enhances voltage stability and power quality. When the demand for reactive power exceeds the available capacity, voltage instability can occur. Factors such as system faults, high loading, and voltage fluctuations can contribute to imbalances in reactive power. To uphold reactive power equilibrium within the system, the integration of FACTS devices along transmission lines enables the injection or absorption of responsive power in accordance with the procedure's needs [6].

The utilization of FACTS brings about several advantages, these benefits include improved power flow control, the benefits of utilizing FACTS devices in operating existing transmission lines include improved safety, mitigation of power oscillations, reduced environmental impact, and the potential for cost savings compared to alternative methods of strengthening transmission systems [7]. Among FACTS devices, the UPFC is useful. [8

The main objective of UPFC is to manipulate the power distribution along the transmission line by implementing a series voltage that autonomously manages both the amplitude and phase angle of the voltage. Through its control over real and reactive power, the UPFC allows for directed power flow on specific paths and improves the capacity of transmission lines, bringing them closer to their thermal limits [9]. Additionally, UPFCs have the capability to enhance power system stability during transient and small signal situations. The UPFC schematic diagram is depicted in Figure 2.

The UPFC is a device that integrates three forms of compensation - impedance, voltage magnitude, and phase angle - to pose a comprehensive result for power system compensation. Through the control of these parameters, the UPFC can achieve complete compensation. Within transmission systems, the UPFC incorporates two separate voltage source converters: one for series conversion and the other for shunt conversion. These convertors are utilized to achieve efficient control over power flow [10]. The UPFC utilizes interconnected converters through a common DC link. The shunt converter, known as the Static Synchronous Compensator (STATCOM), has a dual role: it supplies reactive power to the AC system and provides the required DC power for the inverters. Additionally, the UPFC features a series converter known as SSSC. The SSSC applies a carefully controlled voltage magnitude and phase angle in alignment with the transmission line. Each branch of the UPFC comprises a transformer and a power electronic converter [11].

The UPFC incorporates a shared DC capacitor that serves as an energy storage element, connecting the series and shunt converters. To ensure operational equilibrium in the UPFC, ensuring synchronization between the active power consumption of the shunt converter and the active power generation of the series converter is crucial. Furthermore, the UPFC provides the ability to autonomously regulate reactive power in both the shunt and series converters., resulting in improved flexibility for regulating power flow. A coupling transformer is employed to establish the connection between the device and the power system [12]

1.1. UPFC Literature Review

In the research conducted by [13], a UPFC was designed and simulated for a multi-machine power system. The researchers employed an online design approach utilizing PWM technique to enhance power quality metrics, with voltage drop and increase. The aim of the intended control method in this study is to reduce harmonic distortion within the system while improving voltage oscillations in the DC capacitor. The effectiveness and accuracy of the design are confirmed across simulations done using the PSCAD/EMTDC software

In the study presented in [14], an examination was conducted to assess the influence of integrating UPFC on voltage stability margin and power transfer capacity within a power system. To investigate voltage and power profiles, the

researchers developed a model of a straightforward transmission line system using MATLAB/Simulink and obtained load flow outcomes for an unpaid system. The study subsequently compared these findings with the results obtained after implementing UPFC compensation in the system, emphasizing the enhanced voltage stability margin.

In reference [15], a control scheme was suggested to effectively regulate real power, reactive power, and voltage within a transmission line. This control scheme involved the implementation of a UPFC at the sending end. The efficiency of the suggested control strategy was showcased by conducting computer simulations, showing rapid dynamic response and suitability for enhancing the passing behaviour of the power system during transient conditions.

In reference [16], the concept of D-FACTS was introduced as an economical method for controlling power flow. The study emphasized the UPFC as a highly advanced power electronic system capable of managing power flow in an electrical power system and improving transient stability. A circuit model was formulated for the UPFC, the simulations involved the incorporation of rectifier and inverter circuits, where adjustments were made to the control angle to regulate real and reactive powers at the accepting end.

In reference [17], it was demonstrated how UPFC effectively mitigates harmonics and ensures stability in a grid-connected system utilizing wind energy. The researchers conducted a simulation study utilizing MATLAB/SIMULINK for their investigation.

In [18], a novel modelling approach for the UPFC was proposed, integrating MPC and BFA. The UPFC is an extraordinary device that enables the concurrent management of active and reactive power flows on a transmission line, while enabling voltage regulation at the associated bus. The introduced model, utilizing MPC and BFA, provides a comprehensive insight into the distinctive capabilities of the UPFC and its influence on power system stability. To assess power system stability improvement, a simulation was conducted using MATLAB/Simulink, incorporating a UPFC with an additional PI controller.

The study conducted in [19] evaluated the efficacy of DPFC in compensating the transmission line by employing both PI and fuzzy logic controllers (FLC). The study concluded that DPFC with FLC performs better in compensation than DPFC with PI controller. The DPFC model was simulated using MATLAB/Simulink, and both controllers were implemented and compared using this software

In [20] examined the effect of UPFC on power quality and stability in HVDC transmission systems under various uncertainty conditions The results suggested that incorporating UPFC can improve system performance by effectively controlling power drift in the transmission line. The integration of UPFC results in a reduction in fault current magnitude and mitigates excitation voltage oscillations. Additionally, THD is brought below the IEC standards, rendering the HVDC transmission system more cost-effective for higher power transfer capacity. In [21], a control scheme utilizing an ANN was proposed for employing a UPFC as an active power filter.

The primary objective of the proposed scheme is to ensure the delivery of power to the load while maintaining the desired level of quality. The control unit, incorporating PI controllers optimized using GWO, the scheme continuously observes the voltage at the point where multiple connections are made. The integration of the UPFC enhances power quality by achieving a power factor that tends towards unity, providing fast response times, and enabling the provision of reactive power at low voltage levels. Additionally, the UPFC has the capability to provide voltage compensation. To achieve compensation for unbalanced voltages, two controllers are suggested, utilizing the amplitude of phase voltage and the negative sequence component

2. Shunt–series compensation using a UPFC

Several factors affect the transmission of electric power through an AC transmission line. These factors include the line's impedance, the voltage magnitudes at the sending and receiving ends, and the phase angle between these voltage values. The power flow in a transmission line is significantly affected by variations in voltage about the line impedance. In Figure 1, the transmission line is structured with an inductive reactance (X) and a compensating voltage (U_S). This setup links a voltage source at the distribution-end (U_S) to a voltage source at the receiving-end (U_r).

$$.V_x = V_s + V_{s'_s} - V_r = jIX$$

The transmission line's current is represented as I.

By adjusting the balancing voltage (V_S) linked in series with the transmission line, it is possible to control the voltage (V_X) across the line. This regulation enables the management of both the line current and power flow. The voltage at the transmission line's distribution-end (V_S) precedes the voltage at the reception-end (V_r). As an electrical current (I) passes through the transmission line, it results in the transfer of active power (P_r) and reactive power (Q_r) at the receiving end. To address this, a compensating voltage ($V_{s's}$) is introduced in series with the transmission line.

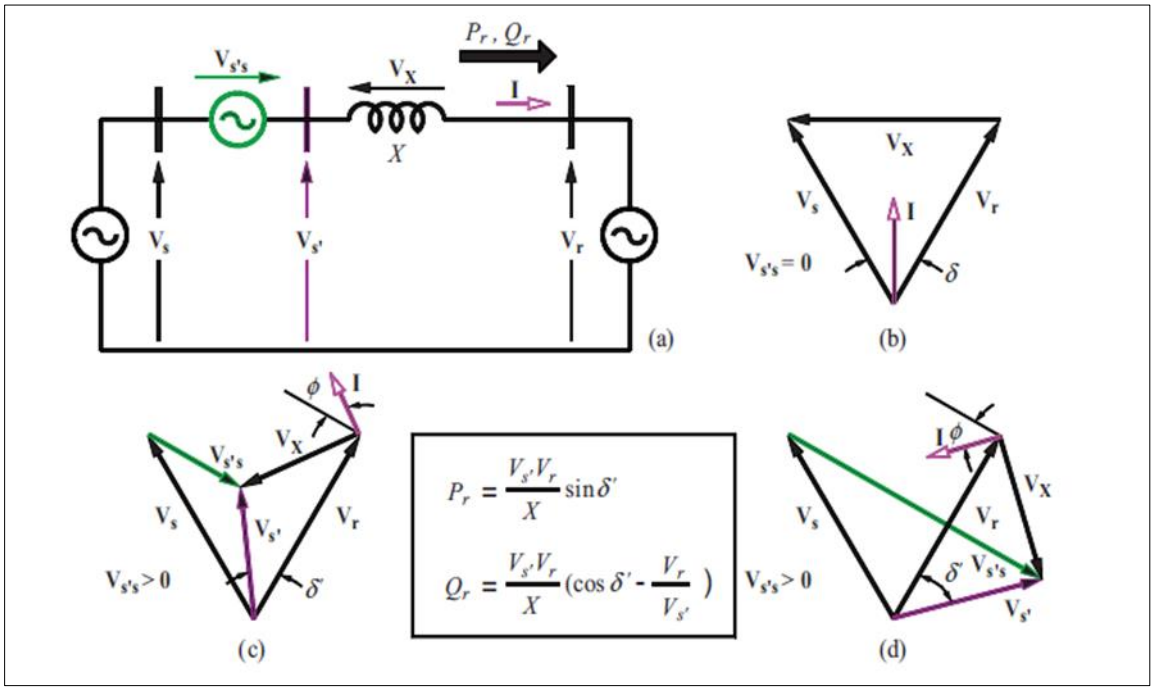

Figure 1 (a) UPFC equivalent circuit. (b) (c) and (d) phasor diagram

Through this modification, the voltage at the sending end ($V_{s'}$) is changed in such a manner that it maintains its lead over the voltage at the reception end (V_r), but with a different phase angle (δ), as illustrated in Figure 1c.

The inclusion of a balancing voltage ($V_{s's}$) in series with the transmission line has a direct influence on the magnitude of power flow and line current, causing them to undergo fluctuations. By modulating the compensating voltage ($V_{s'}$), a phase shift (δ') occurs, causing the voltage at the transmitting end ($V_{s's}$) to lag the voltage at the reception end (V_r), as shown in Figure 1d. This alteration in the voltage relationship triggers a corresponding reversal in both line current and power flow. In Figure 1, the phase angle (∅) concerning the destructive balancing voltage ($-V_{s's} = +V_{dq}$) and the line current (I) can vary from 0 to 2π.

When connected in series with the transmission line, the alignment or misalignment of the negative compensating voltage component with the line current effectively creates a simulated positive or negative resistance. When the perpendicular component of the negative compensating voltage is added in series with the transmission line, it corresponds to either an inductive or capacitive reactance. By adjusting this reactance, it becomes possible to control the transfer of active and reactive powers (P_{exch} and Q_{exch}) between the SSSC and the line.

$$P_{exch} = -V \cdot I = VV_{dq}Icos\varphi$$

and

$$Q_{exch} = |-V_{S'S} \times I| = |V_{dq} \times I|$$

$$= V_{dq}Isin\varphi$$

The STATCOM functions by injecting current at the compensation point, which allows it to either absorb or supply active power to the line. The injected current from the STATCOM consists of an active or direct component (I_d)) that can be

either aligned or misaligned with the line voltage. In addition to the active component, The STATCOM's current delivery includes immediate or quadrature component (I_q) that is orthogonal to the line voltage At the location of compensation, this arrangement effectively replicates either an inductive or capacitive reactance.

By allowing neutral control of the reactive current, it becomes feasible to regulate the voltage at the compensation point. The model for UPFC is illustrated in Figure 2, consisting of dual VSCs interconnected through a common DC link. To ensure practical convenience, the two VSCs are arranged in an identical configuration, which simplifies maintenance and spare parts storage. Each VSC is equipped with an output transformer coupling. The initial VSC, The STATCOM, located at the compensation point, generates a nearly sinusoidal current that can be adjusted in magnitude. Similarly, the SSSC, the second VSC, produces an approximately sinusoidal voltage at the compensation point, connected in series with the line, with the ability to vary its magnitude.

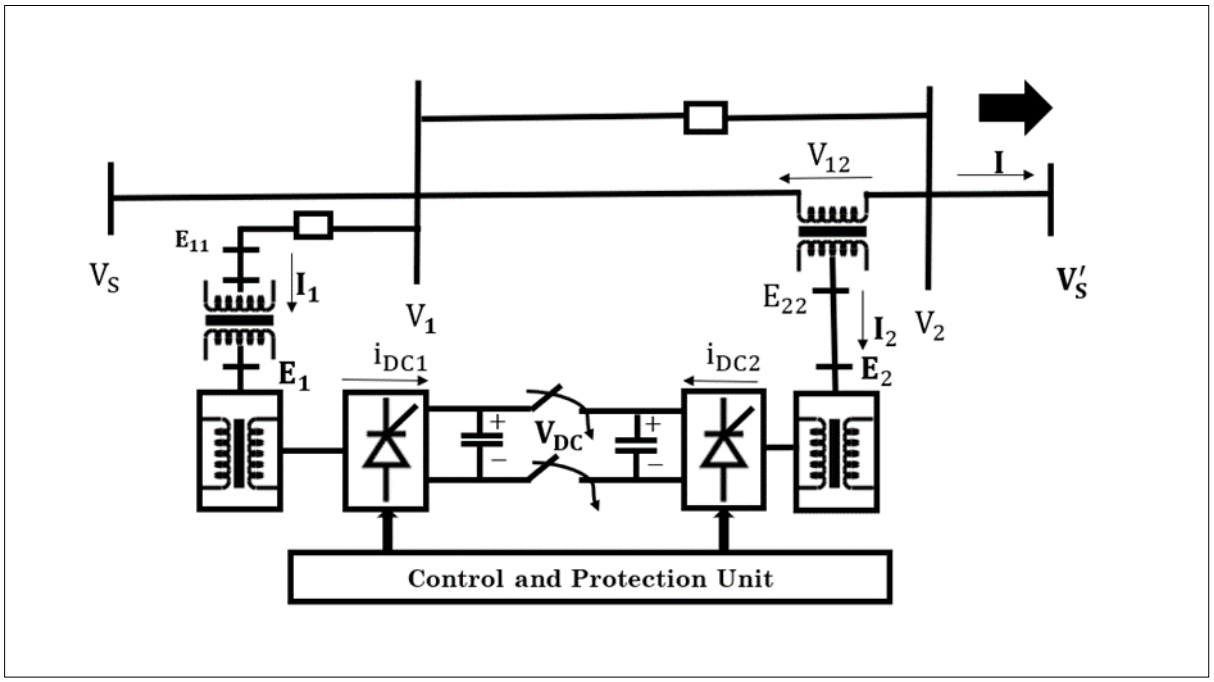

Figure 2 UPFC model

2.1. Control strategy for STATCOM

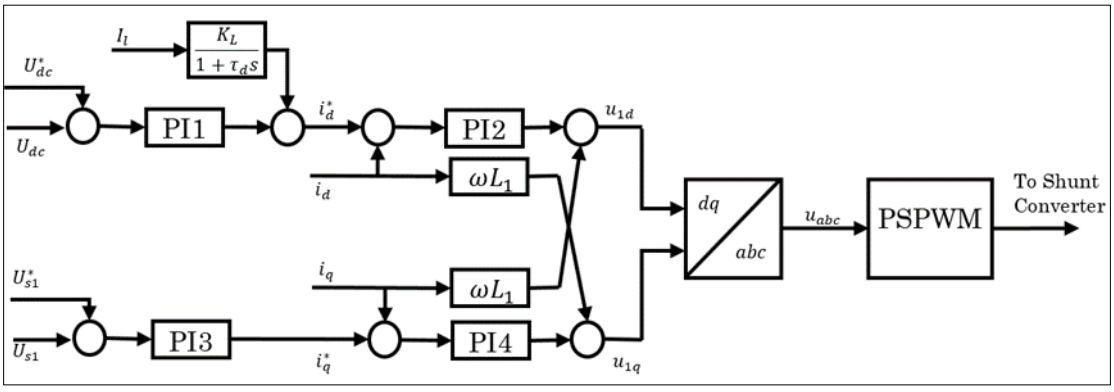

Figure 3 Shunt Inverter Control

The shunt converter, or STATCOM, maintains a constant voltage across the DC link capacitor. At a specified level (U_{dC}=U_{dcref}) by supplying or absorbing the necessary real power for the SSSC.

Moreover, the shunt converter also limits the reactive power in the system. With the rapid dynamics of the shunt inverter's AC currents, it effectively mitigates any undesirable fluctuations in the capacitor voltage. By using a PI

controller in conjunction with the associated shunt current (i_d^* shunt), it is feasible to keep the voltage across the DC bus stable. Likewise, an appropriate reference current i_q^* can be utilized in conjunction with the PI controller to uphold a constant value of the line voltage

$$i_d^* = k_{p1}(U_{dC} - U_{dc}^*) + k_{i1}\int_0^t (U_{dC} - U_{dc}^*)dt + I_l\left(\frac{K_L}{1+\tau_d s}\right)$$

$$i_q^* = k_{p3}(U_{s1} - U_{s1}^*) + k_{i3}\int_0^t (U_{s1} - U_{s1}^*)dt$$

$$u_{1d} = k_{p2}(i_d^* - i_d) + k_{i2}\int_0^t (i_d^* - i_d)dt + i_q\omega L$$

$$u_{1q} = k_{p4}(i_q^* - i_q) + k_{i4}\int_0^t (i_q^* - i_q)dt - i_d\omega L$$

2.2. Control strategy for SCCS

To regulate PQ power in the transmission system, a series inverter is responsible for providing a precise series voltage profile. The output voltages of the inverter are influenced by the time-varying dc-link capacitor voltages, The series inverter utilizes real-time pulse width modulation (PWM) to actively monitor and control fluctuations in the DC-link voltage, thereby reducing their vulnerability to fluctuations caused by line failures.

This confirms that PF imposed by the SCCS remains intact and unaffected by these voltage fluctuations. Failure to generate the required power factors can result in the deactivation of the transmission system. By implementing pulse width modulation (PWM), voltage pulses are carefully controlled to maintain a consistent volt-second mean comparable to the fundamental sinusoidal waveform. Real-time PWM calculation involves selecting a switching period, during which the output voltages VcRd, VcRQ of the series converter utilizes a five-level NPC inverter to generate the pulses that are then fed into the converter

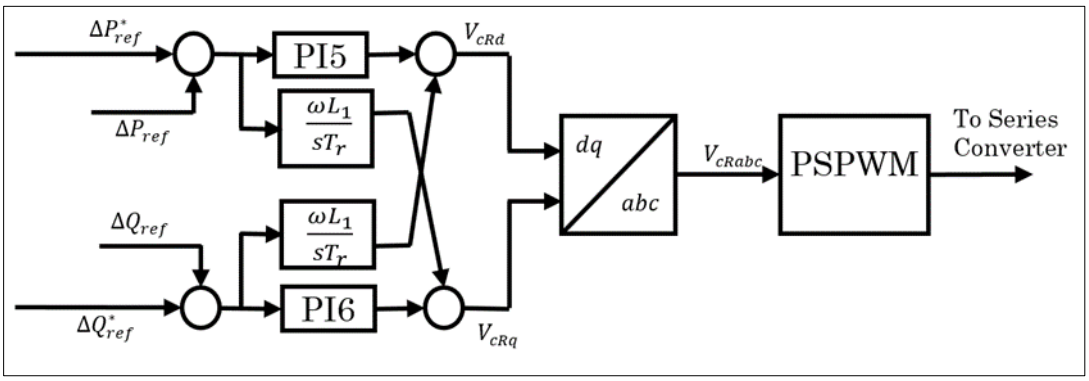

Figure 4 Series converter control strategy

The system employs PI controllers with respective gains of $k_{p1}, k_{i1}, k_{p2}, k_{i2}, k_{p3}, k_{i3}, k_{p4}$, $and\ k_{i4}$ for the shunt converter requires the parameters k_{p5}, k_{i5}, while the series converter relies on the parameters k_{p6}, k_{i6}. However, it should be noted that trial-and-error-tuned PI controllers exhibit larger maximum deviation, reaction time, and in comparison, to other intelligent controllers, this control action is employed when acceptable deviations are permissible, but the presence of offsets is undesirable, as it provides a longer oscillation period. The optimization and tuning of the gains for the PI controllers in the UPFC control system are achieved by utilizing a technique called particle swarm optimization.

3. GWO Optimized PI controlled Five Level UPFC

The GWO optimization technique is applied to enhance the performance of the PI controller utilized in the controller system. GWO optimisation is a modern heuristic algorithm that emulates a simplified social system and has demonstrated effectiveness in resolving continuous nonlinear optimization problems [22]. In comparison to alternative stochastic methods, the GWO technique delivers superior solutions characterized by stable convergence properties and shorter computational time. The proposed approaches are assessed by comparing them to controllers that lack real-

time PWM generation and lack independent control of active and reactive power. This comprehensive evaluation allows for a thorough analysis of their effectiveness

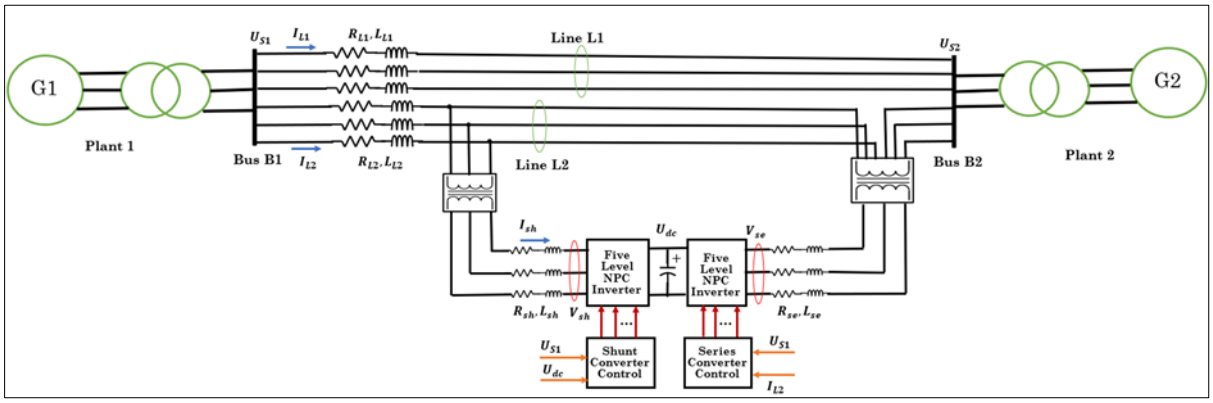

Figure 5 UPFC connected in double circuit transmission line

The PI controller gains, namely k_{p1} , k_{i1}, k_{p2}, k_{i2}, k_{p3}, k_{i3}, k_{i4} *and* k_{p4} for the shunt converter and k_{p5}, k_{i5}, k_{p6}, k_{i6} for the series converter, are optimized through a trial-and-error process. However, this method has some drawbacks such as a longer response time, longer oscillation period, and higher maximum deviation compared to intelligent controllers.

4. Grey Wolf Optimizer (GWO)

4.1. Motivation

Grey wolves (Canis lupus) are apex predators belonging to the Canidae family. Holding the top position in the food chain. Typically, they dwell in packs consisting of approximately 5-12 individuals on average. A noteworthy aspect of grey wolves is their highly structured social hierarchy, as depicted in Figure 6. The pack is led by a dominant male and female, known as alphas, who hold significant decision-making power related to hunting, resting, and waking time, among others. The rest of the pack follows the directives of the alphas.

Apart from adhering to a rigid hierarchy, grey wolves have been observed displaying democratic behaviour, wherein an alpha wolf may follow the guidance of other pack members. During group gatherings, the pack displays recognition of the alpha by lowering their tails as a sign of acknowledgment. The pack members are expected to follow the authority of the dominant wolf, commonly known as the alpha. Additionally, Only the alpha wolf is allowed to mate within the pack, which is intriguing considering that the alpha's leadership is not solely determined by its physical strength, but rather by their exceptional skills in managing and guiding the pack. This underscores the significance of organization and discipline within the pack, which outweigh the importance of physical strength among its members. In the order of grey wolves, the beta wolves occupy the second position and serve as subordinates, assisting the alpha in decision-making and carrying out various pack-related tasks. Irrespective of gender, a beta wolf is considered a potential successor to the alpha position in the event of the death or advanced age of one of the alpha wolves

Although the beta wolf is required to demonstrate respect towards the alpha, they also exert authority over the lower-ranking wolves within the pack. The beta wolf acts as a guide to the alpha, enforcing discipline within the pack and ensuring that the alpha's instructions are followed throughout the group. Additionally, the beta wolf provides feedback to the alpha. On the other hand, the omega holds the lowest rank among the grey wolves. Functioning as a scapegoat, Within the pack, there is a general expectation that the omega wolf submits to all other dominant wolves and is the last one to access food. Despite appearing to hold a subordinate position, the absence of an omega has been observed to cause internal conflicts and challenges for the entire pack. This is because the omega fulfils a crucial role as an outlet for the pack's aggression and frustration. By venting their emotions on the omega, the other wolves can maintain their dominance structure and satisfy the pack's needs. Additionally, in some instances, the omega may also serve as a babysitter for the pack.

Wolves that are not alphas, betas, or omegas are referred to as subordinates (or deltas in some sources). The subordinate wolves are expected to comply with the authority of the alphas and betas, while also exerting dominance over the omegas. Within this group, there are diverse roles fulfilled by individuals, including hunts, patrols, heads,

predators, and caretakers. Scouts are tasked with observing the pack's territory boundaries and promptly notifying the rest of the pack about potential threats or dangers. Sentinels show a crucial role in ensuring the protection and welfare of the pack, serving as guardians and protectors. Elders are seasoned wolves who have previously held alpha or beta positions. Apart from the hierarchical structure, grey wolves demonstrate intriguing social behaviours during group hunting activities. As said by Muro et al., the primary stages of grey wolf hunting can be delineated as follows:

During group hunting, grey wolves display fascinating social behaviours that encompass three primary phases: grey wolves demonstrate their hunting behaviour by tracing, racing, and approach their prey. The wolves engage in persistent pursuit, encircling, and harassing of the prey til it becomes immobilized, after which they launch an attack to secure their meal. In this study, a mathematical model is employed to devise GWO, which integrates the chasing strategies and communal hierarchy of grey wolves to perform optimization tasks

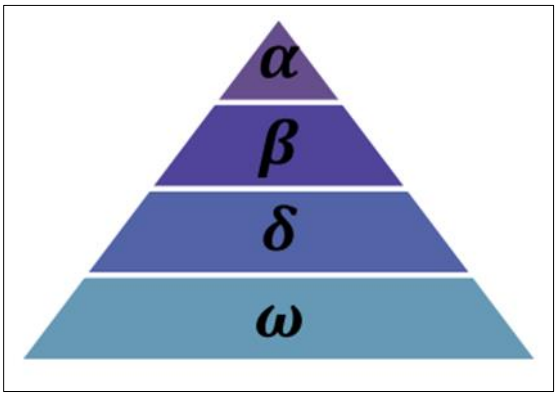

Figure 6 Ranking of grey wolf

4.2. Optimization process

4.2.1. Social hierarchy

During the development of a mathematical model for design the GWO algorithm to create the social hierarchy of grey wolves, distinct ranks are assigned to different solutions. The most superior solution is denoted as alpha (α), while the subsequent positions are occupied by the beta (β) and delta (δ) solutions, representing the second and third fittest results, individually. During the execution of the GWO algorithm for optimization, the hunting behaviour of the wolves is inspired by the actions of the alpha, beta, and delta wolves, while the omega wolves observe and imitate their behaviours.

4.2.2. Encircling prey

Mathematical equations can be employed to represent the encircling behaviours of grey wolves during hunting.

$$\vec{D} = \left|\vec{C}.\vec{X}_p(t) - \vec{X}(t)\right|$$

$$\vec{X}(t+1) = \vec{X}_p(t) - \vec{A}.\vec{D}$$

In the given equations, 't' represents the present iteration. The coefficient vectors are denoted as $\vec{A}$ *and* $\vec{C}$, while $\vec{X}_p(t)$ represents the position vector of the prey. $\vec{X}$ indicates the position vector of a grey wolf.

The vectors $\vec{A}$ *and* $\vec{C}$ are analyzed as follows:

$$\vec{A} = 2\vec{a}.\vec{r}_1 - \vec{a}$$

$$\vec{C} = 2\vec{r}_2$$

The mathematical equations used to model the encircling behaviours of grey wolves during the hunt involve the application of a vector, denoted as $\vec{a}$. The components of this vector gradually reduce from 2 to 0 as the repetitions progress. Moreover, two random vectors, r_1 *and* r_2, are generated with values between 0 and 1. Figure 7(a) illustrates a two-dimensional position vector along with a selection of its potential neighbours, highlighting the impacts of equations (3.1) and (3.2).By adjusting the values of the vectors $\overrightarrow{A}$ *and* $\overrightarrow{C}$, By considering the coordinates of the prey (x^*, y^*), it is possible to observe that a grey wolf positioned at (x, y) can adjust its own position. This enables the wolf to explore various positions around the optimal agent, starting from its current position.

In a search space with multiple dimensions, reaching the location $(x^* - x, y^*)$ can be achieved by configuring the vectors $\vec{A} = (1,0)$ *and* $\vec{C} = (1,1)$.The potential simplified places of a grey wolf in n-dimensional space are represented as geometric shapes, such as hyper-cubes or hyper-spheres, that surround the prey. By leveraging the random vectors r_1 *and* r_2 , the grey wolves gain the ability to explore positions encompassed within the hyper-cubes or hyper-spheres. Consequently, employing equations (3.1) and (3.2), a grey wolf can adjust its position to a random location within the surrounding space near the prey in n-dimensional search spaces

Figure 7 Chasing process of grey wolves

4.2.3. Hunting

When creating an exact representation of the chasing behaviours of grey wolves within an intellectual exploration space, it is crucial to acknowledge the presence of the alpha (best intrant solution), beta, and delta wolves possess a higher level of awareness regarding the potential whereabouts of the optimum (prey). Grey wolves rely on their senses to locate prey and are guided by the alpha, with occasional participation from the beta and delta. However, in the context of optimization, we must rely on mathematical models to simulate these behaviours. To tackle this concern, the GWO algorithm preserves the first three top solutions discovered throughout the optimization process, Considering the enhanced knowledge of the alpha, beta, and delta wolves about the potential optimal solution's location, the remaining search agents, including the omegas, adapt their positions based on the positions of these influential search agents. Mathematically, the suggested formulas are used to represent this behaviour

$$\vec{D}_\alpha = \left|\vec{C}_1.\vec{X}_\alpha - \vec{X}\right|$$

$$\vec{D}_\beta = \left|\vec{C}_2.\vec{X}_\beta - \vec{X}\right|$$

$$\vec{D}_\delta = \left|\vec{C}_3.\vec{X}_\delta - \vec{X}\right|$$

$$\vec{X}_1 = \vec{X}_\alpha - A_1\vec{D}_\alpha$$

$$\vec{X}_2 = \vec{X}_\beta - A_2\vec{D}_\beta$$

$$\vec{X}_3 = \vec{X}_\delta - A_3\vec{D}_\delta$$

$$\vec{X}(t) = \frac{\vec{X}_1 + \vec{X}_2 + \vec{X}_3}{3}$$

Figure 7 illustrates how a search agent adjusts its position within a 2D search space, represented by alpha, beta, and delta. The diagram shows that a search agent's final position is determined by randomly selecting a point within a circle defined by the positions of alpha, beta, and delta in the search space. As a result, alpha, beta, and delta act as estimates of the prey's location, and the other wolves adjust their positions randomly around this estimated prey.

4.2.4. Attacking prey (exploitation)

In the context of the grey wolves' hunting behaviour, it is mentioned that they commence the attack on the prey once it ends stepping. To represent the method of approach the prey, the magnitude of the vector $\vec{a}$ is reduced. Importantly, the vector $\overrightarrow{A}$ reduces the range of fluctuation for $\overrightarrow{A}$. Specifically, $\overrightarrow{A}$ is assigned a random value within the interval [-2a, 2a], with the value gradually decreasing from 2 to 0 as the iterations progress. In the GWO algorithm, search agents can move closer to the prey by utilizing random values of $\overrightarrow{A}$ within the range of [-1, 1].

This is shown in Fig. 8(a), where the magnitude of $|A| < 1$, indicating movement towards the prey. Despite the effectiveness of the proposed operators in guiding the search agents on the prey, the GWO algorithm may become trapped in local optima. Although the encircling mechanism provides some degree of exploration, additional operators are required to promote exploration.

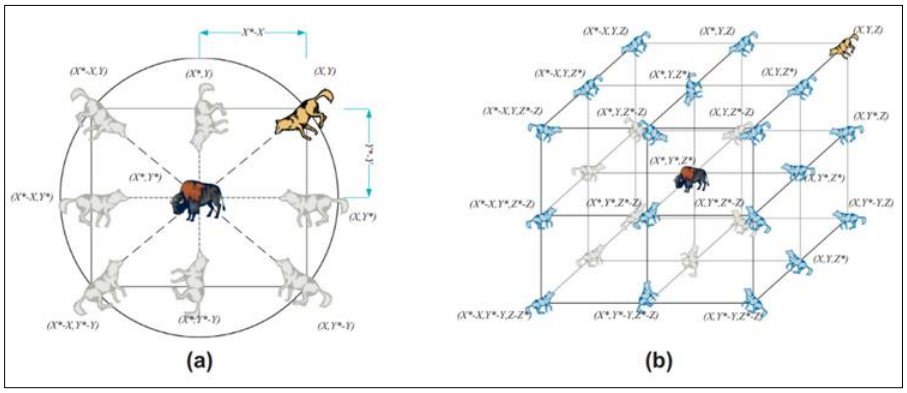

Figure 8 Present Position and next position of the vectors

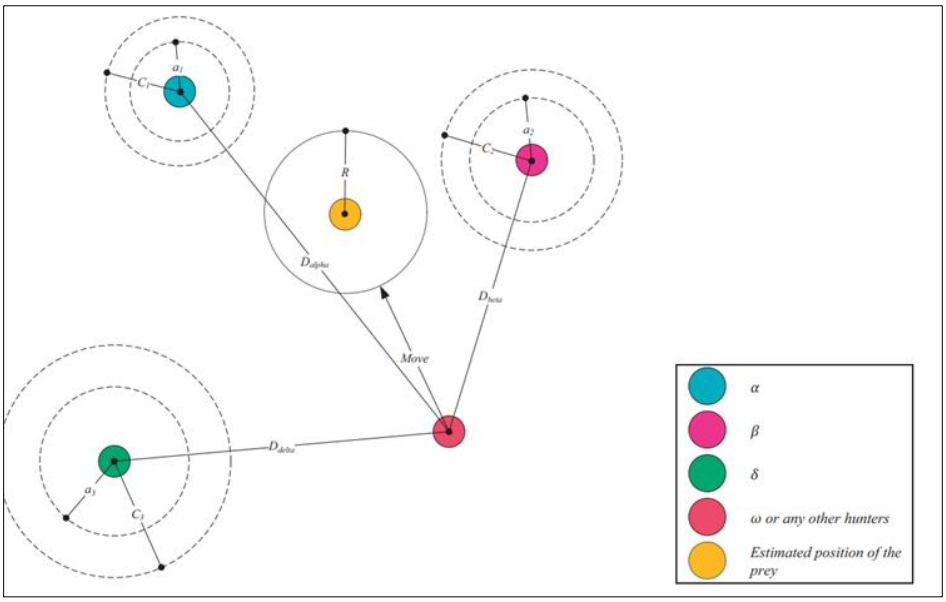

Figure 9 Shifting of position vectors

4.2.5. Search for prey (exploration)

In the GWO algorithm, grey wolves prioritize tracking the locations of alpha, beta, and delta as their main objective. However, they also actively explore their surroundings to minimize the risk of getting stuck in local optima. To facilitate this objective, the algorithm incorporates the notion of divergence by employing $(A)^{\rightarrow}$ with randomly assigned values exceeding 1 or falling below -1. This prompts the search agents to deviate from their current target and explore the entirety of the search space. The figure depicted in 9(b) demonstrates that when the magnitude of $|A|>1$, the grey wolves steer away from their prey, thereby enhancing the chances of unearthing a superior global solution.

The GWO algorithm also incorporates an exploration component represented by the vector $(C)^{\rightarrow}$.As described in Equation (3.4), this vector comprises random values within the interval [0, 2], emphasizing the exploration aspect of the algorithm. By assigning arbitrary weights to the prey, $(C)^{\rightarrow}$can amplify the influence (when $C > 1$) or diminish the influence (when $C < 1$) of the prey's effect on determining the distance in Equation (3.1).

The purpose of incorporating this element into GWO is to enhance its optimization process by promoting exploration and preventing the convergence to local optima.

It is crucial to note that unlike A, C does not decrease linearly over the course of the algorithm. Instead, it consistently introduces random values throughout the entire process. This feature serves to emphasize exploration, not only in the early stages but also in the later stages of optimization. This component proves particularly beneficial in overcoming instances of stagnation in local optima, especially towards the end of the iterations. The presence of this component proves highly advantageous when encountering stagnant local optima, particularly

during the concluding iterations. Moreover, apart from its exploration function, the C vector can effectively mimic the obstacles that wolves face when pursuing their prey in the wild. These obstacles impede the wolves' smooth and rapid progress towards their target, analogous to the role of C within the GWO algorithm.

The GWO algorithm initiates the search process by creating a set of candidate solutions represented by grey wolves. In each iteration, the alpha, beta, and delta wolves make educated estimates of the prey's potential location by considering the current best solutions. Additionally, the $A^{\rightarrow}$ and $C^{\rightarrow}$vectors play important roles in the search process by allowing wolves to converge and diverge around the prey, and by stochastically emphasizing or de-emphasizing the presence of the prey significantly influences the distance calculation. These components collectively empower the GWO algorithm to efficiently explore and find optimal solutions across a range of optimization problems. Initially, candidate solutions are randomly initialized, and in each iteration, the alpha, beta, and delta wolves estimate the potential position of the prey. To achieve a balance between exploration and exploitation, every candidate solution adjusts its proximity to the prey by gradually decreasing the parameter "a" from 2 to 0. When the magnitude of $|A^{\rightarrow}|>1$, candidate solutions exhibit a tendency to move away from the prey, exploring the seek space. Conversely, when the magnitude of $|A^{\rightarrow}<1|$, candidate solutions converge towards the prey, exploiting the best solutions. Eventually, the algorithm concludes based on a predetermined termination criterion.

The provided pseudo code for the GWO algorithm offers a comprehensive insight into its functionality and its ability to address optimization problems. It is important to highlight the following key aspects

- The social hierarchy in GWO aids in preserving the best solutions achieved throughout the iterations, which can be represented as hyper-spheres expanding to higher dimensions.
- The encircling mechanism establishes a neighbourhood in a circular shape around the solutions.
- The hunting method proposed enables candidate solutions to accurately identify the apparent location of the prey. which can be represented as hyper-spheres expanding to higher dimensions.
- The randomly chosen factors A and C contribute to candidate solutions possessing hyper-spheres with varying radii.
- The adaptive values of parameters "a" and "A" in GWO algorithm maintain a balanced trade-off among search and use. By reducing "A", GWO dedicates half of the repetitions for searching ($|A| \geq 1$) and the remaining half for use ($|A| < 1$).
- GWO simplifies the parameter adjustment process by only requiring adjustments to two main parameters: a and c.

In future research, there is potential to investigate the integration of mutation and other evolutionary operators into the GWO algorithm, aiming to ape the

complete life cycle of grey wolves. This expansion would broaden the capabilities and applicability of the algorithm. However, it is worth noting that the GWO algorithm intentionally maintains simplicity, limited to a few adjustable operators. The inclusion of these mechanisms could offer further avenues for improving the algorithm's performance and are thus suggested for future investigation

4.3. Pseudocode of GWO algorithm

Pseudocode of GWO algorithm
• Set the number grey wolves or candidates and maximum iterations. • Choose the values for $\boldsymbol{a}, \vec{\boldsymbol{A}}$ **and** $\vec{\boldsymbol{C}}$ • for $\boldsymbol{i = 1}$ **to** number of candidates • using random numbers set initial candidates within the limits of maximum and minimum values. • end for • Calculate the fitness value of every candidate. • Rank the candidates according to fitness values. Choose first best, second best and third best solutions. • While (iterations<maximum number of iterations) do • for $\boldsymbol{i = 1}$ **to number of candidates** • renew the candidates position • end for • calculate $\boldsymbol{a}, \vec{\boldsymbol{A}}$ **and** $\vec{\boldsymbol{C}}$ • calculate the fitness value by every candidate and rank the candidates • find the position of $\boldsymbol{X_\alpha}, \boldsymbol{X_\beta}$ and $\boldsymbol{X_\delta}$ • update the iteration number. • end while

To attain maximum control overactive and reactive power, and voltage regulation, within the UPFC control system, it is crucial to effectively handle both the shunt converter and series converter. To achieve this, it becomes essential to establish distinct values for six proportional gains (K_{p1} *to* K_{p6}) and six integral constants (K_{i1} *to* K_{i6}). Optimizing the performance of the shunt and series VSI controls in the power system depicted in Figure 5 requires careful consideration of these parameters.

To enhance the efficiency of the shunt and series VSI controls utilized in the depicted power system (see Figure 5), there is a need for improvement. It is essential to enhance their performance, it is essential to determine specific parameters. These parameters include six proportional gains (K_{p1} *to* K_{p6}) and six integral constants (K_{i1} *to* K_{i6}))). Their determination is vital for optimizing the control system's effectiveness.

In pursuit of this goal, various performance metrics are employed, the measurements encompass various parameters, such as discrepancies in active and reactive power, the magnitude of voltage, the voltage of the DC link, and the current. The optimization of the twelve parameters is accomplished using GWO algorithm. A population of twenty GWO particles is chosen to ensure stable dynamic and transient control of the UPFC, contributing to a stable and robust UPFC control system. Lastly, PSO algorithm is applied to minimize the cost function.

$$Cost = \sum_{t=0}^{20000} \left(\begin{array}{c} \sqrt{(\Delta P_{error}(t))^2} + \sqrt{\left(\Delta Q_{error}(t)\right)^2} + \\ \sqrt{\left(\Delta U_{dc}(t)\right)^2} + \sqrt{\left(\Delta U_{s1}(t)\right)^2} + \sqrt{\left(\Delta i_d(t)\right)^2} + \sqrt{\left(\Delta i_q(t)\right)^2} \end{array} \right)$$

The cost function used in the optimization process involves the active power error Δp_{error}, reactive power error ΔQ_{error}, DC link voltage error ΔU_{dc}, voltage magnitude error ΔU_{S1}, as well as the direct and quadrature axis current errors Δi_d *and* Δi_q

5. Simulation results

Simulations are functioned to confirm the operational efficacy of UPFC control system. which is based on a five-level NPC topology and optimized using the GWO algorithm. The simulations are conducted utilizing the test network model illustrated in Figure 10and the parameters specified in Table 1. The system consists of generators that incorporate three-phase synchronous machines. Additionally, it includes exciters, hydraulic turbine-driven governors, power stabilizers, and an output transformer. The chosen configuration for the test transmission network emulates a transmission line with two parallel circuits, comprising two parallel 220-kV subsystems, to form a system section

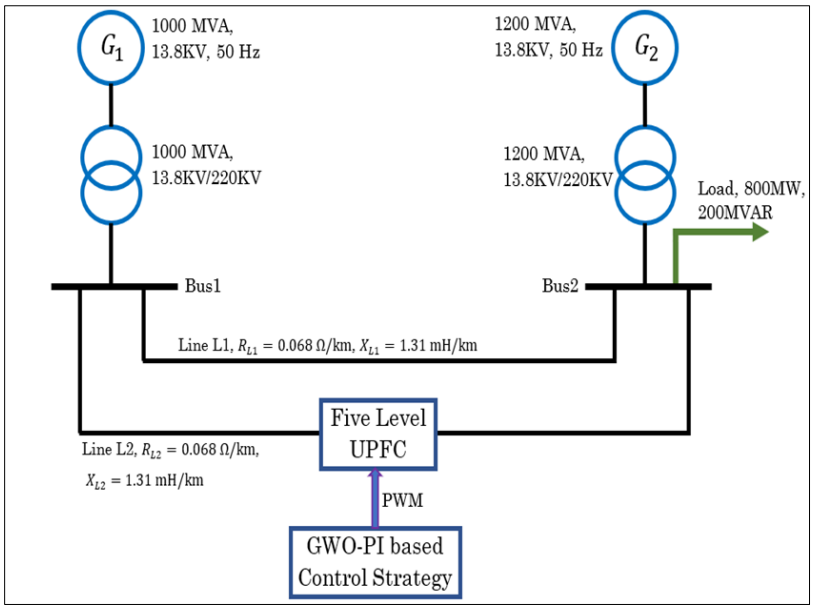

Figure 10 Test System with UPFC

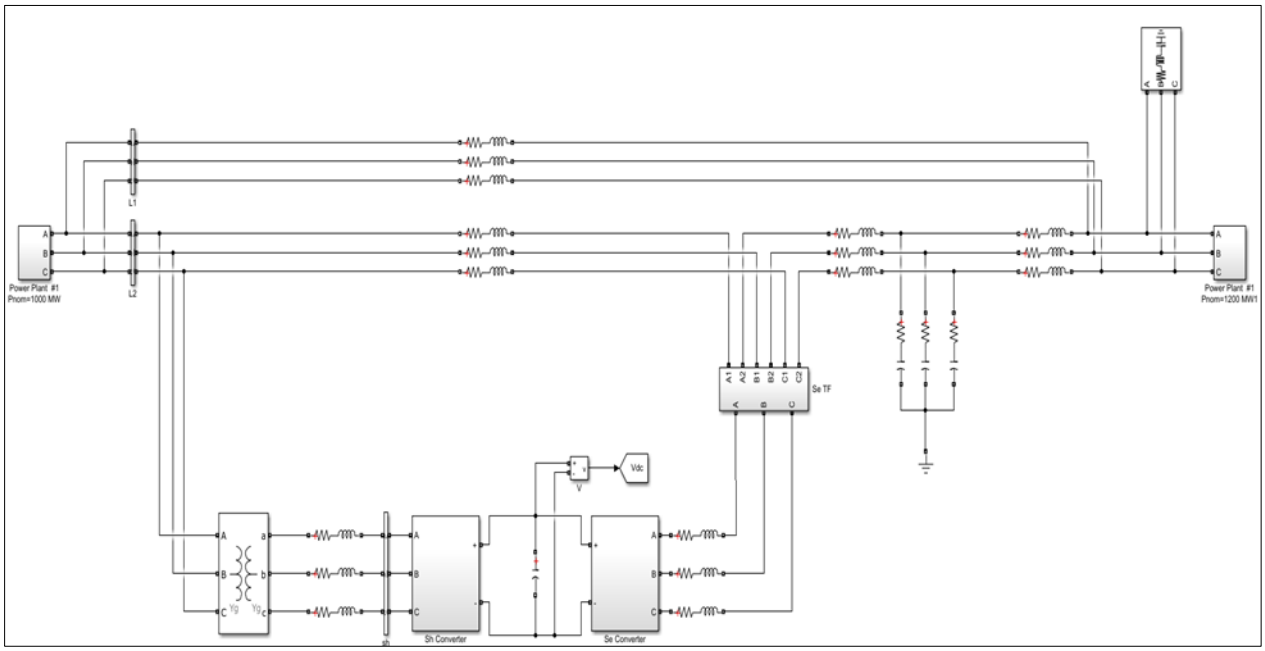

Figure 11 UPFC Simulation

Table 1 Parameters of the test System

Sending end	Synchronous Machine 1000MVA, 13.8KV, 50Hz Transformer 1000MVA, 13.8KV/220KV
Receiving end	Synchronous Machine 1200MVA, 13.8KV, 50Hz Transformer 1200MVA, 13.8KV/220KV
Line L1	Resistance 0.068 Ω/km Inductance 1.31 mH/km Capacitance 0.00885 μF/km Line Length 65km
Line L2	Resistance 0.068 Ω/km Inductance 1.31 mH/km Capacitance 0.00885 μF/km Line Length 65km
UPFC	DC Link Voltage 56KV DC Link Capacitors each 750μF Shunt Converter rating 100MVA Series Converter rating 100MVA

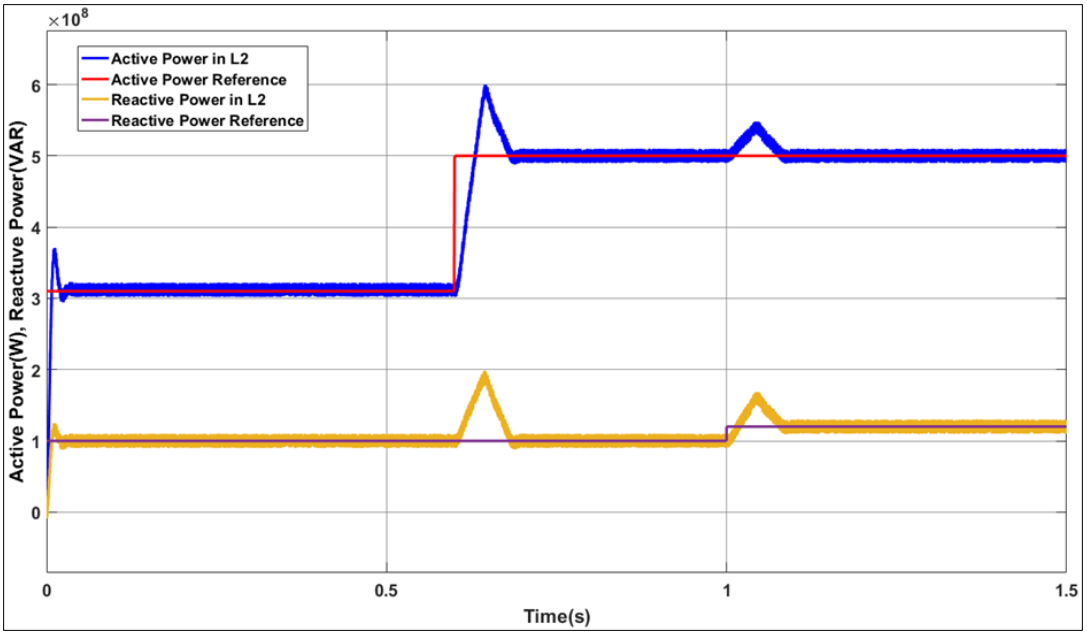

(a)

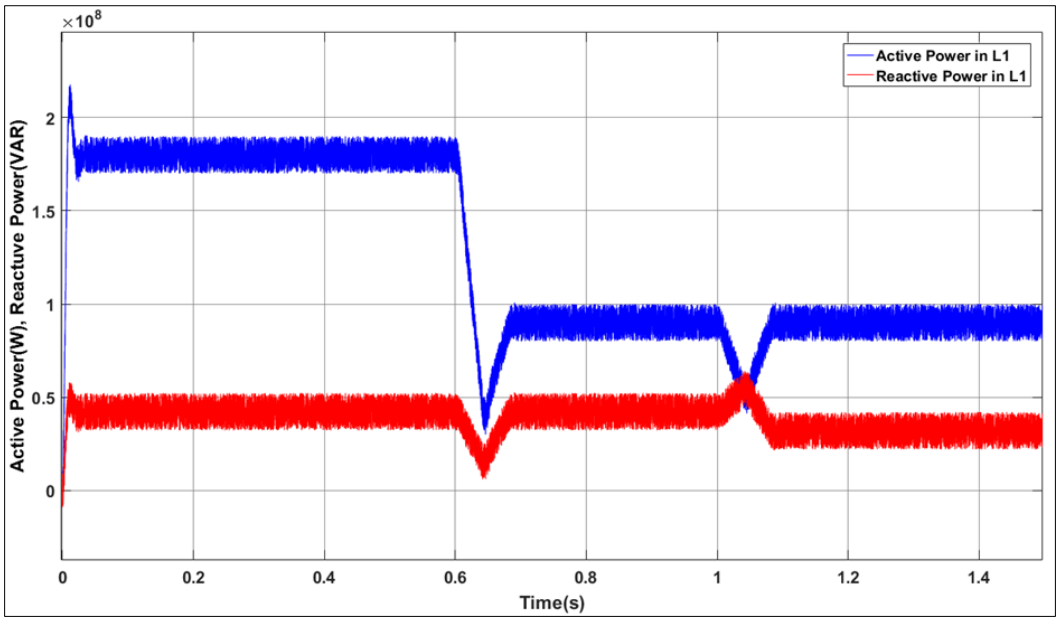

(b)

Figure 12 Conventional PI controlled UPFC (a) power variation in L2 (b) power variation in line L1

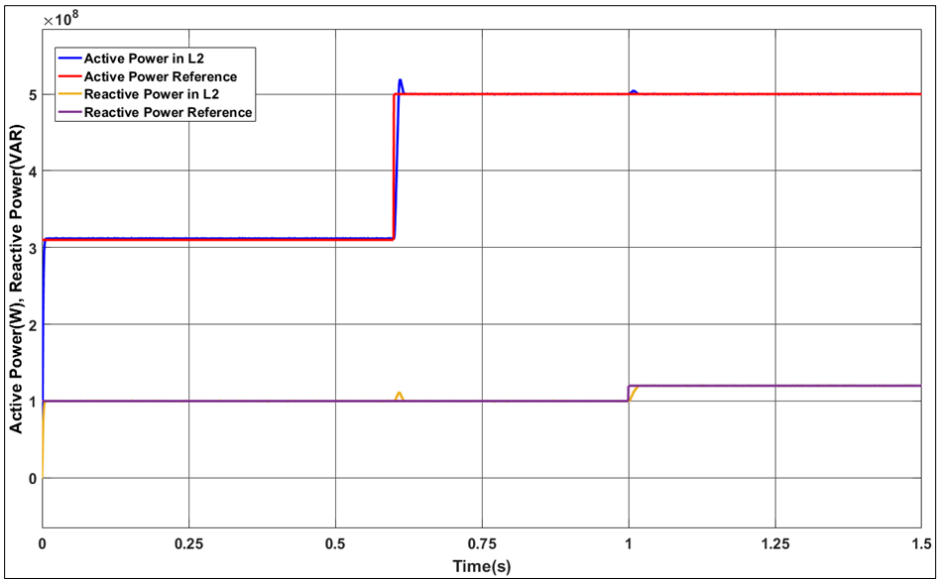

(a)

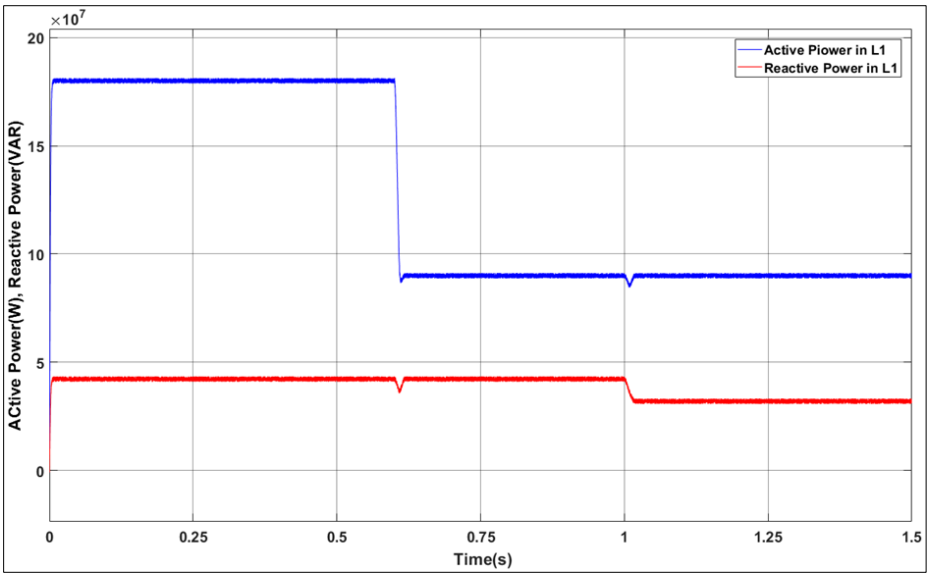
×10^7
Active Piower in L1
Reactive Power in L1
ACtive Power(W), Reactive Power(VAR)
Time(s)

(b)

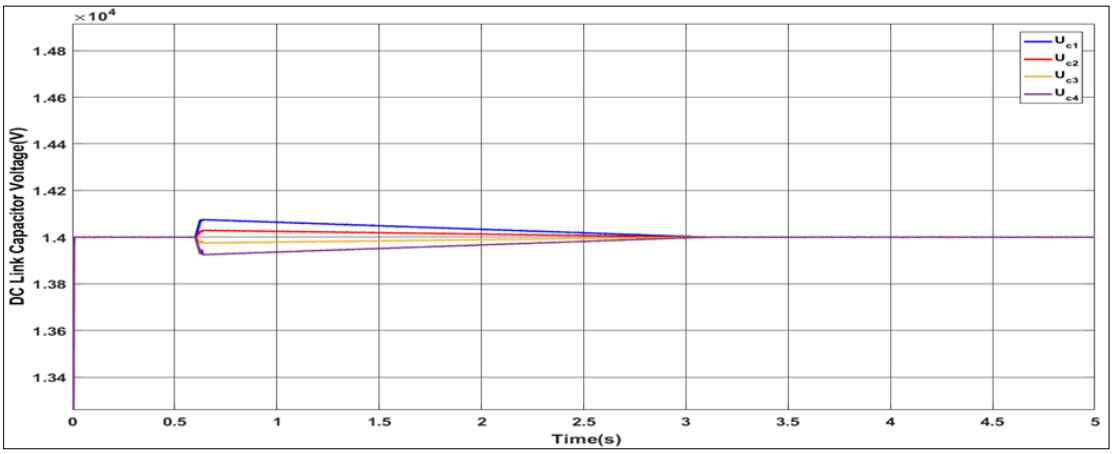
×10^4
DC Link Capacitor Voltage(V)
Time(s)

(c)

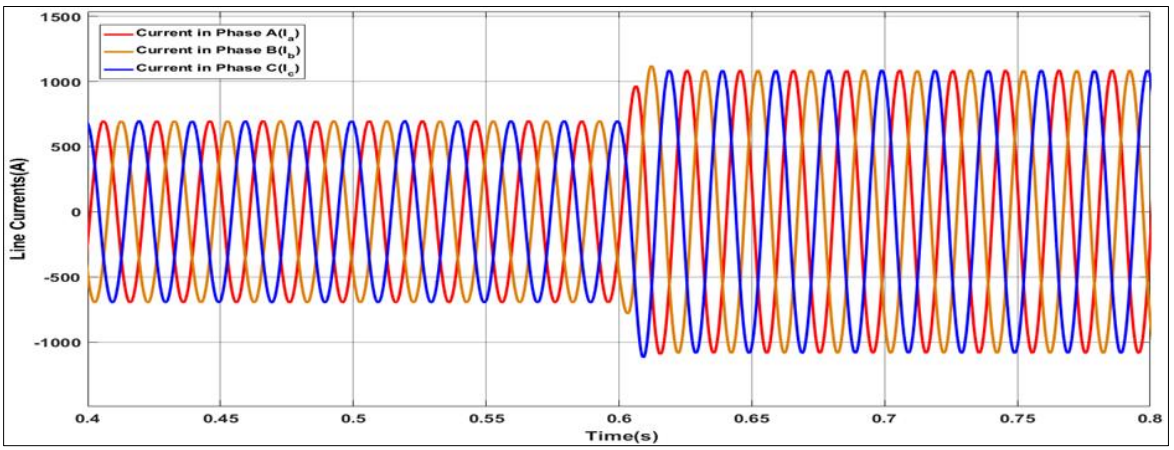
Current in Phase A(I_a)
Current in Phase B(I_b)
Current in Phase C(I_c)
Line Currents(A)
Time(s)

(d)

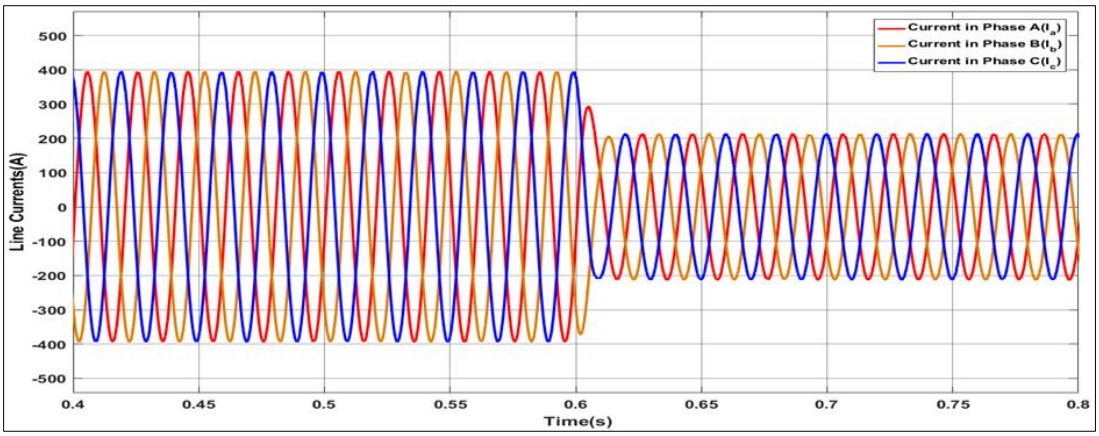

Figure 13 GWO optimized PI controlled UPFC (a) power variation in line$\mathbf{L_2}$, (b) power variation in one of the $\mathbf{L_1}$ lines, and (c) voltage across the DC link (d) currents through line L1 (e) currents through line L2

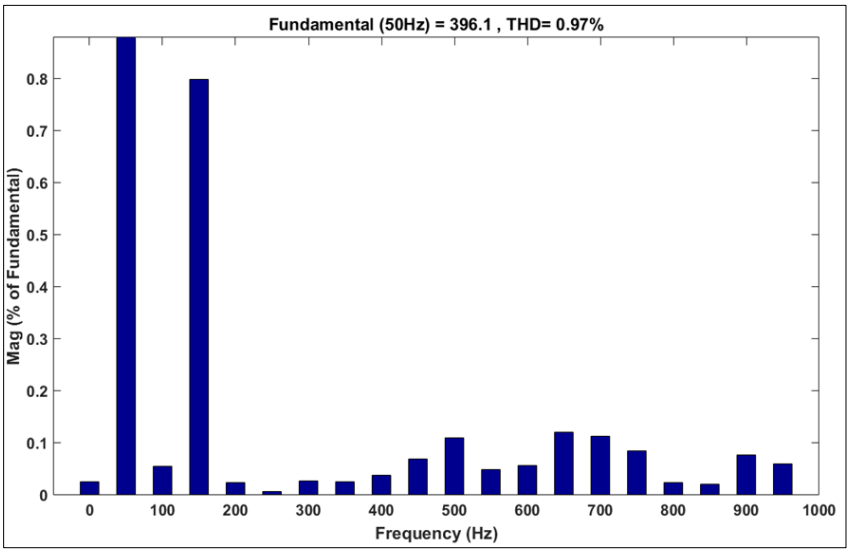

(a)

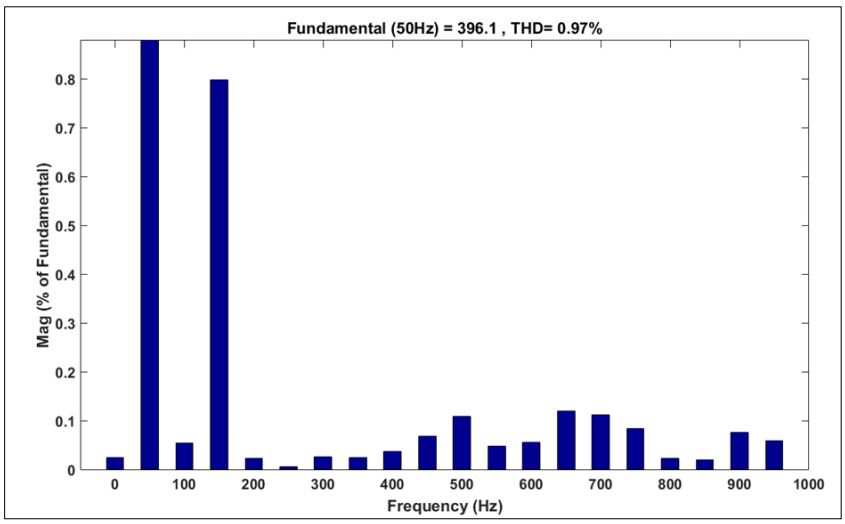

(b)

Figure 14 the current THD in L1 and L2

To maintain a balanced power flow across the dual circuit transmission line, the UPFC is positioned between buses 2 and 4 on Line 2. The primary goal of the system is to effectively control and regulate the power flow on Line 2, thereby ensuring efficient management of the power flow on Line 1. The UPFC utilizes two Five-level Neutral Point Clamped converters arranged in a continuous configuration, performing the roles of both series and shunt converters. To generate the required switching pulses for these converters, a phase shifted PWM technique is utilized. To regulate the series converter, the phase-shifted pulse width modulation (PSPWM) relies on the reference waveforms are generated through DC voltage control and line voltage magnitude control for the UPFC. On the other hand, the shunt converter utilizes reference waveforms made from active and reactive power control to operate through PSPWM. The controllers and converter models integrated into the network; the Matlab/Simulink environment was utilized. The simulation focused on analysing the dynamic response of the system, specifically the second 220-kVline, when exposed to a sudden alteration in active and reactive power references, while in the influence of the UPFC control.

Initially, the active power value was set to P = 312 MW and the reactive power reference to Q_ref = 90.00 MVAr. At t = 0.6 s, a step change is introduced, setting P_ref to 500.00 MW, followed by another step change at t = 1 s, adjusting Q_refto 120.00 MVAr. The double circuit transmission line undergoes testing with the UPFC, utilizing PI controller gains that have been adjusted through the iterative process of trial-and-error. The specific values of these gains can be found in Table 1. Figure 12(a) depicts the dynamic power flow in line L2, while Figure

12(b) exhibits the reactive power flow in line L1. Notably, both figures exhibit a peak overshoot of 20% and demonstrate a stability time of 0.12 seconds.

The PI controller utilized in the UPFC exhibits insufficient performance in peak overshoot and stability time, potentially resulting in system instability under vibrant conditions. The tracking capability of the PI controllers is enhanced by utilizing the GWO to optimize the controller gains. By drawing lessons from the hierarchical structure and cooperative hunting strategies observed in grey wolves, we can derive insights for application in various contexts., the proposed approach optimized the gains by following the guidelines specified in Table 2. Figure 15(a) presents the behaviour of active power flow in Line L2, while Figure 15(b) illustrates the behaviour of reactive power flow in Line L1.

In Figure 15(c), the diagram shows the difference in electrical potential across the capacitors of the DC link in the five-level multilevel inverter. Furthermore, Figure 15(d) represents the currents in Line L1, while Figure 15(e) represents the currents in Line L2. Figure 16 illustrates THD of the line currents in Line L1 and L2. Figure 13 clearly shows that the UPFC significantly enhances the ability to accurately track active and reactive power on Line L2, as indicated by the reduced peak overshoot and stability time.

During the simulation, at the 0.6-second mark, a three-phase fault occurred on the 220-kV double line (L2). The fault was subsequently resolved and cleared at 0.64 seconds, assuming that there was a temporary interruption in the line. Three distinct scenarios were examined, and the corresponding Figures 15, 16, and 17 illustrate the active and reactive power flow in Line L1 and L2 for each scenario. The considered scenarios consist of three cases: without UPFC, with a PI-controlled UPFC operating under normal conditions, and with a PI-controlled UPFC optimized using GWO. Figure 13(a) shows the active power flow in Line L1, which runs parallel to the faulty Line L2, without the implementation of UPFC. Additionally, Figure 13(b) demonstrates the reactive power flow in Line L1 under identical circumstances.

In the three-phase fault, the transmitted power experienced a significant decrease, approaching zero. However, once the fault was cleared, Line L1 became overloaded due to the power flow redistribution. The multilevel UPFC enables efficient control of the active and reactive power flows in Line L1 by utilizing Line L2 for regulation. In Figures 16(a) and 16(b), we can observe the active and reactive power flow in Line L1 and Line L2, respectively, when employing a conventional PI controller. On the other hand, Figures 17(a) and 17(b) depict the active and reactive power flow in Line L1 and Line L2, respectively, when utilizing a PI controller optimized with the GWO algorithm. These figures demonstrate that, following the clearance of the fault, The UPFC effectively controlled the power transfer in Line L1, ensuring that both the active and reactive power stayed within the capacity limits of the line. Figure 18, the performance of the PI

controller optimized by GWO in dynamic scenarios, particularly when subjected to fluctuations in active and reactive power. The active power experiences consecutive changes at time instances of 0, 0.6, 1.5, 2.2, and 3 seconds, the values for active power vary sequentially at time instances of 0, 1, 2, 3, and 4 seconds, with respective magnitudes of 310 MW, 500 MW, 400 MW, 300 MW, and 500 MW. Likewise, the reactive power undergoes successive changes at time instances of 0, 1, and 3 seconds, with corresponding magnitudes of 100 MW, 150 MW, and 100 MW. Figure 14 demonstrates the effectiveness of the proposed GWO-optimized PI controller in accurately tracking these changes, resulting in reduced peak overshoot and firmness time.

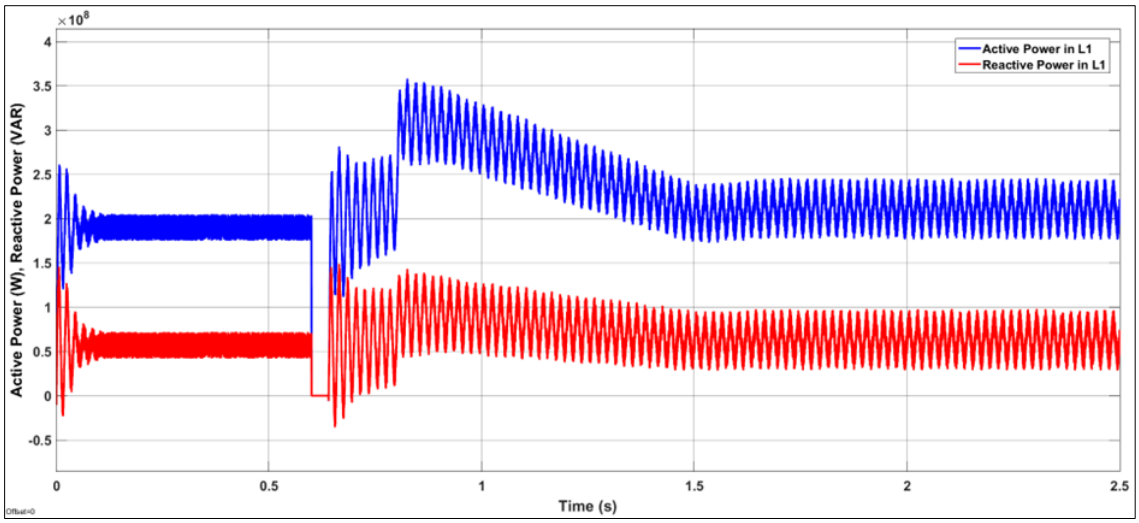

(a)

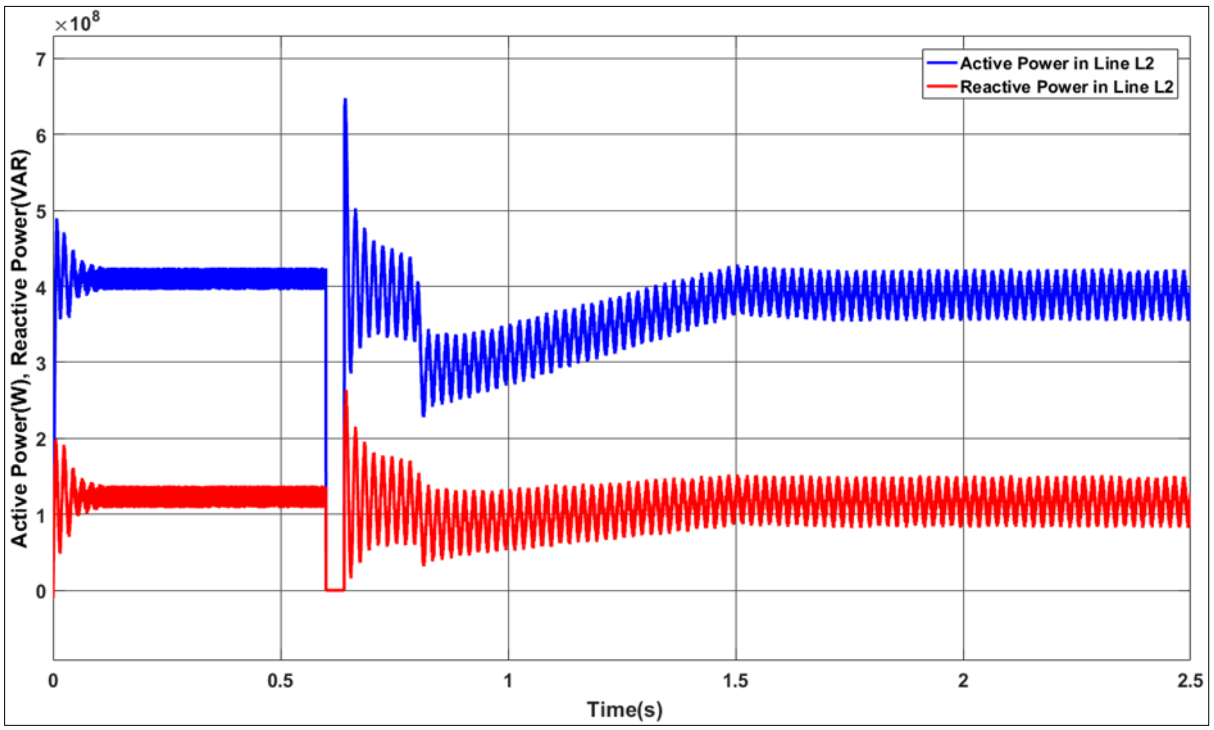

(b)

Figure 15 Power variation in L1 and L2 not connecting UPFC

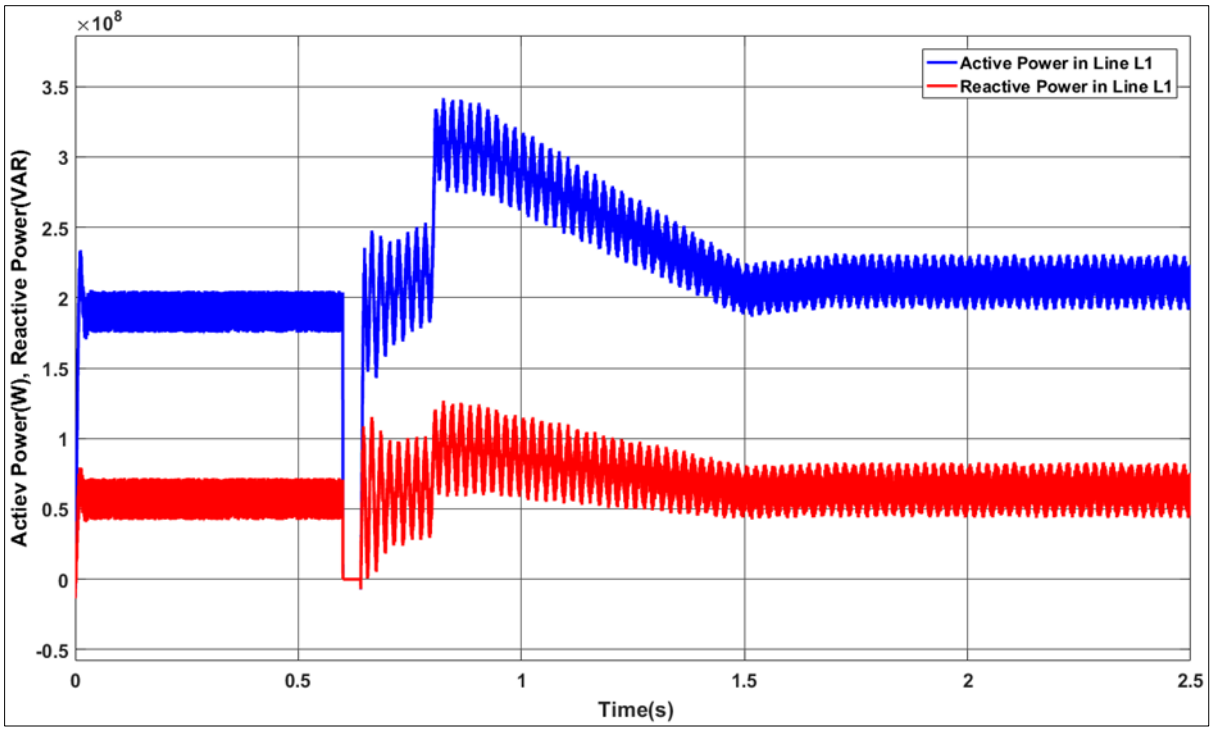

(a)

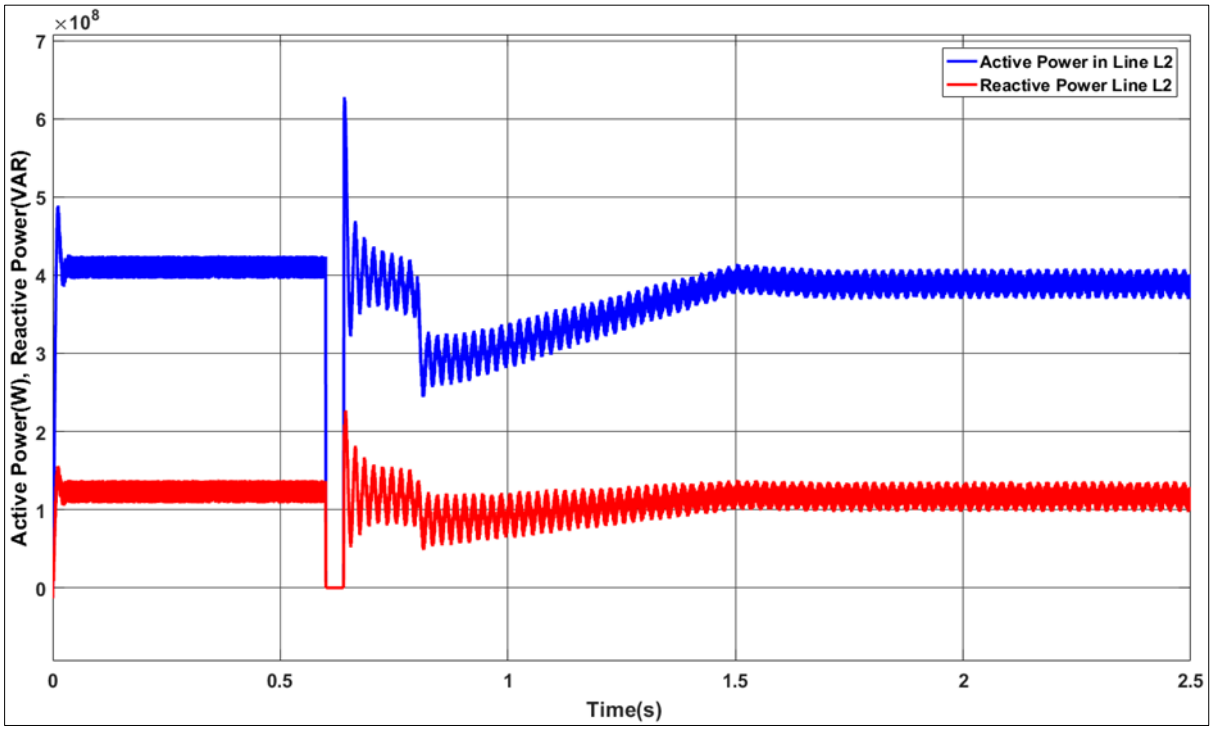

(b)

Figure 16 Change in power in L1 and L2 with PI regulator UPFC

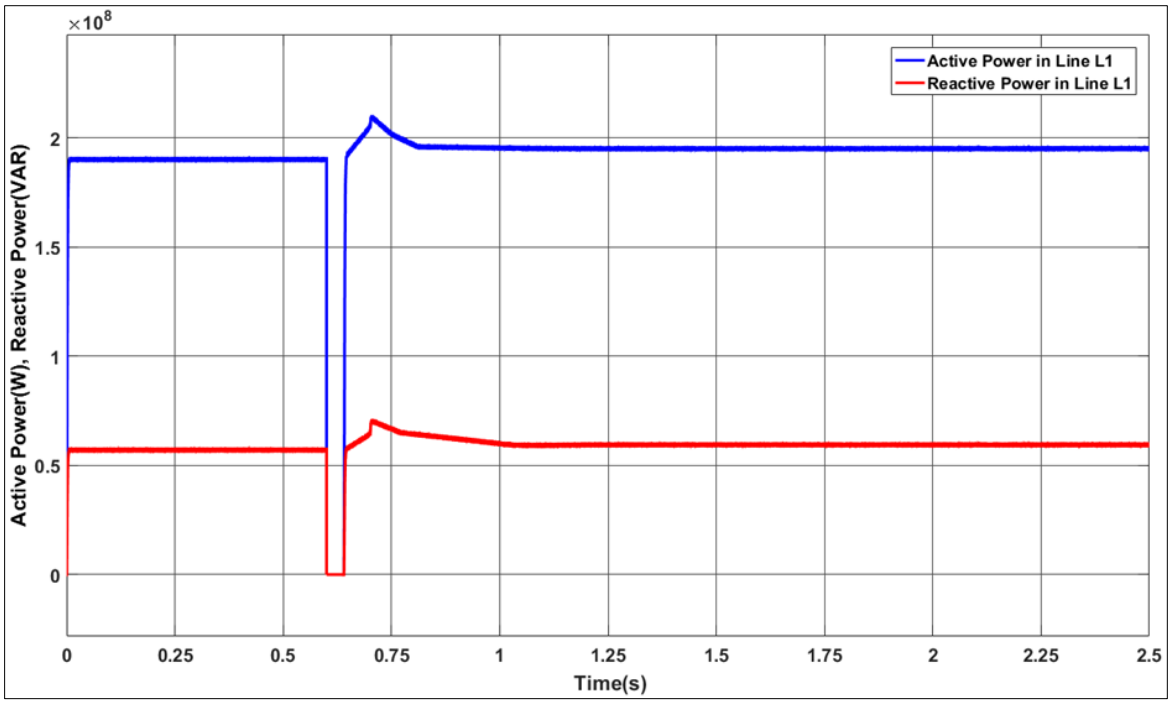

(a)

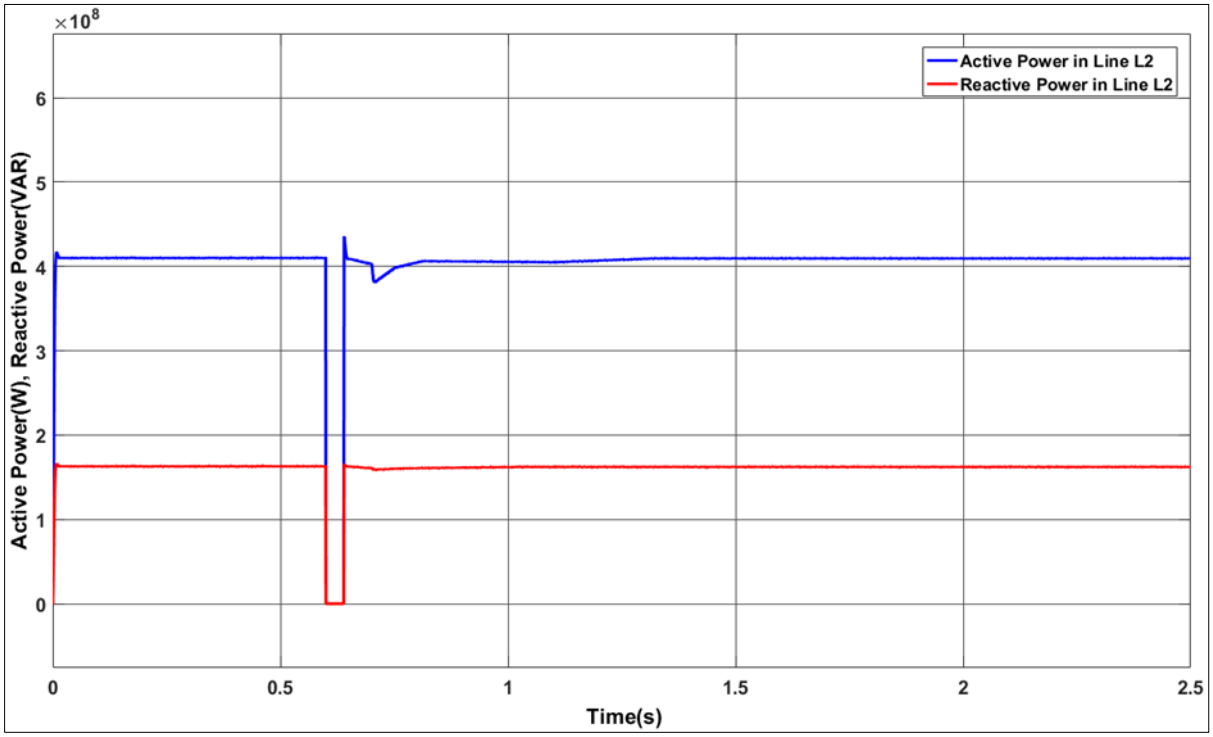

(b)

Figure 17 Change in power in L1 and L2 through GWO tuned PI regulator UPFC

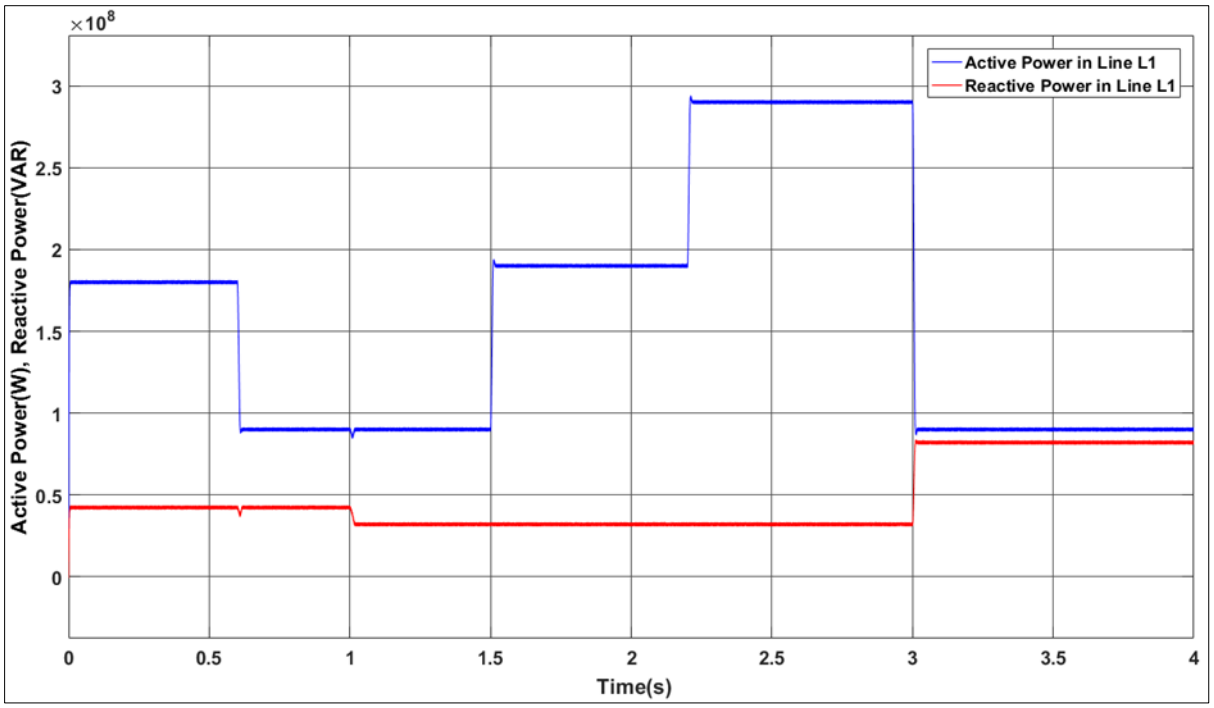

(a)

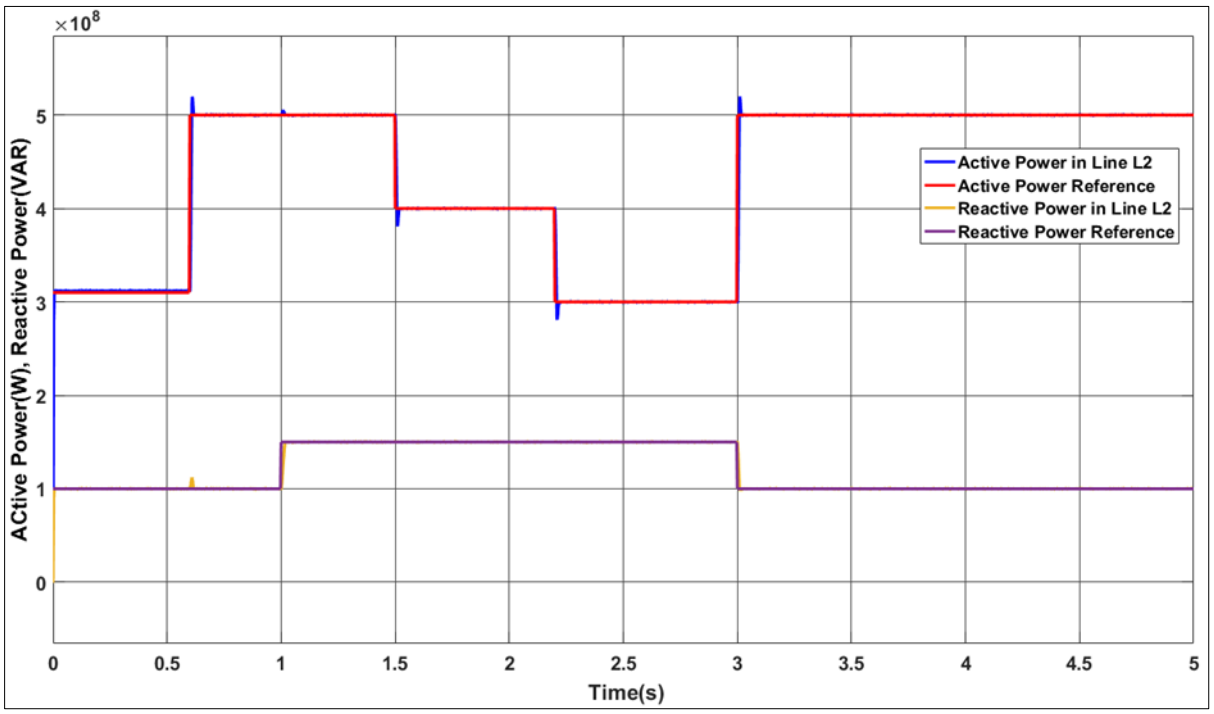

(b)

Figure 18 Change in power in L1 and L2 line

Table 2 PI Control Gains

Using Trial and Error method	Kp1=0.1285, Kp2=0.6740, Kp3=1.0852, Kp4=0.9052, Kp5=2.3851 Kp6=1.1850 Ki1=6.7581, Ki2=10.0857, Ki3=3.8570, Ki4=2.0745 Ki5=3.6857, Ki6=5.0745
Using GWO optimization	Kp1=0.0135, Kp2=0.1958, Kp3=0.8044, Kp4=0.9875, Kp5=2.8077 Kp6=0.7095 Ki1=7.4251, Ki2=14.0147, Ki3=4.4785, Ki4=2.1085 Ki5=6.1785, Ki6=4.4089

6. Conclusion

Within this, GWO-based optimization approach is employed to finely change the PI controller of the UPFC. The main objective is to efficiently control the active and reactive power flow in a double-circuit transmission line. The configuration of the UPFC system consists of two interconnected multilevel converters. More specifically, the five-level NPC converters are organized in a configuration where they are connected back-to-back. Functioning as both shunt and series converters. The UPFC control strategy proposed in this study comprises three key components. First, active, and reactive power are controlled independently. Second, real-time Pulse Width Modulation (PWM) generation is employed in both multilevel converters of the UPFC system. The gains for controlling the dc-link voltage in these converters are intentionally designed to minimize their sensitivity to changes in the dc link current.Finally, maintaining the balance of the dc-link capacitor voltages is achieved by utilizing both the series and shunt multilevel converters. The proposed UPFC control technique ensures the balanced voltages of the dc-link capacitors by effectively utilizing both converters. This approach differs from the conventional method that typically balances the voltages using only one of the converters. The approach incorporates separate control of active and reactive power, real-time Pulse Width Modulation (PWM) creation in both convertors, and dc-link voltage control gains designed to be less affected by changes in dc link current. The outcomes demonstrate clear improvements in performance through the proposed technique, along with the optimization of PI controller gains using GWO. This approach effectively enhances the tracking capability of active and reactive power flow.

Compliance with ethical standards

Disclosure of conflict of interest

No conflict of interest to be disclosed.

References

[1] Kumar, R. S., Raj, I. G. C., Saravanan, S., Leninpugalhanthi, P., & Pandiyan, P. (2021). Impact of power quality issues in residential systems. In Power Quality in Modern Power Systems (pp. 163-191). Academic Press.

[2] Satapathy, Anshuman, Niranjan Nayak, and Tanmoy Parida. "Real-Time Power Quality Enhancement in a Hybrid Micro-Grid Using Nonlinear Autoregressive Neural Network." Energies 15, no. 23 (2022): 9081

[3] Asija, D., & Viral, R. (2021). Renewable energy integration in modern deregulated power system: challenges, driving forces, and lessons for future road map. In Advances in Smart Grid Power System (pp. 365-384). Academic Press.

[4] Nwaigwe, K.N., Mutabilwa, P. and Dintwa, E., 2019. An overview of solar power (PV systems) integration into electricity grids. Materials Science for Energy Technologies, 2(3), pp.629-633.

[5] Al-Badi, A.H., Ahshan, R., Hosseinzadeh, N., Ghorbani, R. and Hossain, E., 2020. Survey of smart grid concepts and technological demonstrations worldwide emphasizing on the Oman perspective. Applied System Innovation, 3(1), p.5.

[6] Hariharasudan, A., Otola, I. and Bilan, Y., 2020. Reactive power optimization and price management in microgrid enabled with blockchain. Energies, 13(23), p.6179.

[7] Liu, Qiang, Songlin Sun, Bo Rong, and Michel Kadoch. "Intelligent reflective surface based 6G communications for sustainable energy infrastructure." IEEE Wireless Communications 28, no. 6 (2021): 49-55.

[8] Upadhyay SK, Yadav PK, Bhasker R, Kumar SV. INFLUENCE OF FACTS DEVICES ON ELECTRICAL TRANSMISSION SYSTEM.

[9] Choudhury, S., Saçiak, A. and Hanson, J., 2022. Communication-free decentralized power flow control of unified power flow controllers and phase-shifting transformers in high voltage transmission systems. IET Generation, Transmission & Distribution.

[10] Huang H, Zhang L, Oghorada O, Mao M. Analysis, and control of a modular multilevel cascaded converter-based unified power flow controller. IEEE Transactions on Industry Applications. 2020 Oct 7;57(3):3202-13.

[11] Zhao, X., Bai, P., Zhang, C., Zhao, Z., Wang, X. and Guo, X., 2022. Analysis and validations of operation behaviors for dual active bridge-based unified power quality conditioner under different working conditions. International Journal of Circuit Theory and Applications.

[12] Navlakha M, Choudhary A, Jangid J, Meena M, Khandelwal H, Bansal L. Power Flow Control in Transmission System with the use of UPFC.

[13] Rajderkar, V.P. and Chandrakar, V.K., 2023. Design Coordination of a Fuzzy-based Unified Power Flow Controller with Hybrid Energy Storage for Enriching Power System Dynamics. Engineering, Technology & Applied Science Research, 13(1), pp.10027-10032.

[14] Shahzad, U., 2021. Impact of Synchronous Condensers on Power System Static Voltage Stability Considering Line Contingencies in the Presence of Renewable Generation. arXiv preprint arXiv:2111.11423.

[15] Anas, M., Badgaiyan, P. and Jain, D., 2022. A Comparative Study of UPFC Controlled with Programmable Integral Controller and RL Controls. Research Journal of Engineering Technology and Medical Sciences (ISSN: 2582-6212), 5(04).

[16] Fatule, Eduardo J. Castillo, Jose F. Espiritu, Heidi Taboada, and Yuanrui Sang. "A Computationally Efficient Evolutionary Algorithm for Stochastic D-FACTS Optimization." In 2020 52nd North American Power Symposium (NAPS), pp. 1-6. IEEE, 2021.

[17] Saidi, Youcef, Abdelkader Mezouar, Mohammed Amine Benmahdjoub, Brahim Brahmi, Atallah Meddah, Bouhafs Khalfallah, and Kamel Djamel Eddine Kerrouche. "A Comprehensive Review of LVRT Capability and Advanced Nonlinear Backstepping Control of Grid-Connected Wind-Turbine-Driven Permanent Magnet Synchronous Generator During Voltage Dips." Journal of Control, Automation and Electrical Systems 33, no. 6 (2022): 1773-1791.

[18] Singh, B., Slowik, A. and Bishnoi, S.K., 2023. Review on Soft Computing-Based Controllers for Frequency Regulation of Diverse Traditional, Hybrid, and Future Power Systems. Energies, 16(4), p.1917.

[19] Ahilan, T. (2023). Wind connected distribution system with intelligent controller-based compensators for power quality issues mitigation. Electric Power Systems Research, 217, 109103

[20] Darabian, M., Bagheri, A. and Yousefi, S., 2023. Design of a new robust controller for voltage regulation of DC link in wind-farm-side converter integrated with a hybrid AC and DC large-scale power system. IET Generation, Transmission & Distribution.

[21] Thumu, R., Harinadha Reddy, K. and Rami Reddy, C., 2021. Unified power flow controller in grid-connected hybrid renewable energy system for power flow control using an elitist control strategy. Transactions of the Institute of Measurement and Control, 43(1), pp.228-247